ACTA METALLURGICA SLOVACA
2024, VOL. 30, NO. 2, 57-63

RESEARCH PAPER

THERMODYNAMIC DIAGRAM ANALYSIS AND SMELTING OF COMPLEX Fe-Cr-Mn-Si FERROALLOY

Serik Gabdullin[1], Yerbolat Makhambetov[1], Zhalgas Saulebek[1], Amankeldy Akhmetov[1], Zulfiadi Zulhan[2], Gulsana Mukhtarkhanova[3], Ruslan Toleukadyr[1], Kuandyk Dyussenbekov[4]*

[1]Laboratory of Ferroalloys and reduction processes, Zh. Abishev Chemical-metallurgical institute, Ermekov 63, Karaganda city, Kazakhstan
[2]Metallurgical Engineering Department, Faculty of Mining and Petroleum Engineering, Institut Teknologi Bandung, Jl. Ganesa No. 10, Bandung 40132, Indonesia
[3]Research Institute "INNTECH", 018 accounting quarter building 22/1, Karaganda city, Kazakhstan
[4]The National University of Science and Technology MISIS, Leninskiy Prospekt 4, Moscow, Russia

*Corresponding author: makhambetovyerbolat@gmail.com, tel.: +7 771-517-2882, Laboratory of Ferroalloys and reduction processes / Zh.Abishev Chemical-metallurgical institute, 100009, Karaganda, Kazakhstan

Received: 15.04.2024
Accepted: 21.05.2024

ABSTRACT

A state diagram of the Cr-Mn-Si-Fe metallic system, which simulates the compositions of complex chromium-manganese-silicon-containing ferroalloy (Fe-Cr-Mn-Si), has been constructed using thermodynamic-diagram analysis. Theoretical investigations have determined that the system comprises eight elementary tetrahedra. The sum of the relative volumes of the elementary tetrahedra equals one (1.00000), confirming the accuracy of the tetrahedration conducted. Analytical expressions for each tetrahedron have been derived. Calculations have determined the tetrahedron characterizing the phase composition of the ferroalloy. This tetrahedron is identified as the most voluminous phase triangle in the Cr-Mn-Si-Fe metallic system, implying that its significant volume facilitates the smelting process of chromium-manganese-silicon-containing ferroalloy, i.e., there is the possibility of freely regulating the charge compositions to achieve the required alloy grade. Based on the obtained results, an experimental smelting of the Fe-Cr-Mn-Si ferroalloy was conducted using a charge composed of chromium ore, low-grade manganese ore, and coke, resulting in a sample with the following composition, %: 44.07 Cr, 13.97 Fe, 12.48 Mn, 9.48 Si, 4.45 C. The microstructure comprises a complex silicide (Cr, Fe, Mn)$_3$Si and Cr_3C_2 carbides.

Keywords: diagram, chromium, manganese, silicon, phase, Hize's method, complex ferroalloy

INTRODUCTION

An analysis of the global raw material base for metallurgy indicates a diminishing supply of high-quality ore while the demands for metal quality are increasing. This trend necessitates materials with new complex properties, including ferroalloys of complex composition. The chromium-manganese-silicon-containing ferroalloy Fe-Cr-Mn-Si is particularly interesting, as it includes the most common and widely used alloying elements in steel smelting. Their combination allows for more efficient use of Fe-Cr-Mn-Si in alloying steels and alloys due to better assimilation in steel [1-5]. Another advantage is the possibility of involving raw materials of lower quality, low-grade ores and slags in producing such ferroalloys [6-9].

However, the complexity of the composition and the multi-component nature of the charge for smelting Fe-Cr-Mn-Si complicate the control of the smelting process [6]. In metallurgy theory and practice, studying the state of materials involved in metallurgical conversion, depending on temperature and pressure, is significant. Conducting in-depth physicochemical research, which provides a theoretical foundation, is critically important for improving metal quality and implementing new promising technologies, based on which further smelting trials can be more easily controlled [10, 11].

Yet, classical thermodynamic studies of processes in complex systems require complex mathematical calculations and the determination of thermodynamic parameters for many independent reactions [12-14].

Multiple interdependent thermodynamic processes occur simultaneously in complex systems, especially those involving chemical or phase changes. Each reaction has its own set of conditions and constraints, contributing to the system's overall behaviour. Analyzing these reactions requires solving sets of nonlinear differential equations describing how these processes interact, significantly complicating the calculations.

For complex systems, determining the stability of phases or reaction products involves minimizing Gibbs free energy across all possible states. This computational task becomes exponentially more demanding as the number of components and potential phases increases, often requiring sophisticated algorithms and significant computational resources.

These aspects make classical thermodynamics a highly complex field, particularly when applied to new complex materials [15-18].

Thermodynamic-diagram analysis offers a solution to the dilemma of researching processes in metallurgy. This method is efficient when applied to metallurgical technology, as it reveals the characteristics of phase states of raw materials involved in metallurgical conversion. Ultimately, such research results in a phase diagram of a particular system that closely approximates the compositions of metallurgical products. From this diagram, one can visually track the evolution of phase transformations in slag and metallic systems and predict their final state [19, 20].

The present work aims to reveal phase transformation regularities in metallic systems based on Fe, Cr, Mn, and Si. A phase composition diagram of the four-component Cr-Mn-Si-Fe system and a mathematical model for assessing the nature and quantity of the secondary phases formed within it have been constructed. This system characterizes the compositions of the complex Fe-Cr-Mn-Si ferroalloy, which is obtained from chromium and low-grade manganese ores using the carbothermic method and is used for the deoxidation and alloying of steel.

In conclusion, integrating thermodynamic modelling with empirical testing is imperative to improve the understanding of phase transformations in metallic systems based on Fe, Cr, Mn, and Si. Such research is necessary to support the development of new technologies and to adapt to the raw material constraints faced by the metallurgy industry while achieving high-quality metal production.

For this purpose, smelting Fe-Cr-Mn-Si from chromium and low-grade manganese ores of Kazakhstan and Coke has been conducted based on modelling results.

METHODS OF THERMODYNAMIC MODELLING

In this study, thermodynamic modelling was conducted using a theoretical (computational) method to construct phase composition diagrams, which were mathematically described using a balanced method.

For conducting a tetrahedration of the Cr-Mn-Si-Fe system using the thermodynamic diagram analysis method, it is necessary to delineate the boundary subsystems Fe-Mn-Si, Fe-Cr-Si, Cr-Mn-Si, and Cr-Mn-Fe. This process utilizes the principle of Gibbs free energy minimization. If, when writing the reaction for interaction between phases, the change in Gibbs energy was negative, then the reaction products as coexisting phases on the diagram were connected by a straight line. The consecutive implementation of this operation leads to the acquisition of a diagram of equilibrium coexisting phases. To accomplish this, it is first required to describe the metallic associations of various complexities that constitute the system under consideration.

1. The *Fe-Cr-Si* system consists of three binary subsystems: Fe-Cr, Cr-Si, and Fe-Si. No binary compounds have been identified in the Fe-Cr subsystem, while the Cr-Si subsystem contains four chromium silicides: Cr_3Si, CrSi, Cr_5Si_3, and $CrSi_2$. Among these, CrSi melts incongruently. The Fe-Si binary subsystem has five Fe silicides: Fe_5Si_3, $FeSi_2$, FeSi, Fe_3Si, and Fe_2Si, three of which (Fe_5Si_3, $FeSi_2$, and Fe_3Si) also melt incongruently and were thus excluded from the construction of the diagram. The congruently melting compounds identified have melting points ranging from 1212 to 1770 °C. Triangulation of the Fe-Cr-Si system (see **Fig. 1**) revealed six thermodynamically stable regions (Fe-Cr_3Si-Cr, Fe-Fe_2Si-Cr_3Si, Fe_2Si-Cr_3Si-FeSi, FeSi-Cr_3Si-Cr_5Si_3, FeSi-Cr_5Si_3-$CrSi_2$, FeSi-$CrSi_2$-Si).

2. The *Fe-Mn-Si* system comprises three binary subsystems: Fe-Mn, which has no binary compounds since manganese and iron are known to be completely soluble in each other in solid state.; Mn-Si, which contains four manganese silicides: Mn_5Si_3, MnSi, $Mn_{11}Si_{19}$, and Mn_3Si. The latter two melt incongruently and were not included in the diagram construction. The Fe silicides of the Fe-Si system were listed previously. Thus, four congruent compounds (FeSi, Fe2Si, Mn5Si3, MnSi) were identified in this three-component metallic subsystem. Using the thermodynamic-diagram analysis method, this system (**Fig. 2**) is divided into five stable regions (Fe-Mn-Fe_2Si; Mn-Fe_2Si-Mn_5Si_3; Fe_2Si-Mn_5Si_3-MnSi; Fe_2Si-MnSi-FeSi; MnSi-FeSi-Si).

3. In the triangulation conducted on the *Cr-Mn-Si* system (**Fig. 3**), six thermodynamically stable regions were identified (Mn-Cr_3Si-Cr; Mn_5Si_3-Cr_3Si-Mn; MnSi-Cr_3Si-Mn_5Si_3; Cr_5Si_3-MnSi-Cr_3Si; $CrSi_2$-MnSi-Cr_5Si_3; Si-$CrSi_2$-MnSi). This system also includes the three binary subsystems: Cr-Mn, Cr-Si, and Mn-Si. The first subsystem lacks binary compounds, while the Cr and Mn silicides in the second and third subsystems were previously described in two of the ternary systems. Thus, the system contains five congruent compounds (Cr_3Si, Cr_5Si_3, $CrSi_2$, Mn_5Si_3, and MnSi).

4. The *Cr-Mn-Fe* system consists of three binary subsystems: Cr-Mn, Mn-Fe, and Cr-Fe. None of these three binary systems have binary compounds (refer to **Fig. 4**). This suggests a straightforward solubility between these three metals without forming intermediate solid solutions or compounds at the represented conditions.

Fe and Cr are known to be mutually soluble in each other, forming solid solutions over a wide range of compositions. This solubility is because Fe and Cr are both body-centered cubic (BCC) at room temperature and have similar atomic radii, which allows them to dissolve in one another without significant lattice distortion. The complete solubility occurs in the α-phase (BCC) at lower temperatures and in the δ-phase (also BCC) at higher temperatures. Mn and Fe also exhibit a wide range of solubility. Mn can dissolve in Fe at room temperature to form a solid solution. Cr and Mn also have solubility in each other, though to a lesser extent than in Fe.

The solubility between Cr, Mn, Fe and Si is more complex due to the formation of various silicides. In a binary sense, Si generally has limited solubility in these metals, and the systems are characterized by forming several distinct silicides at different compositions like M_3Si, M_5Si, MSi and MSi_2.

A phase composition diagram of the Cr-Mn-Si-Fe system was constructed using a similar analysis method across all triangles of the four ternary subsystems. Consequently, the studied phase equilibria of the quaternary metallic system Cr-Mn-Si-Fe, which models the compositions of various grades of the complex Fe-Cr-Mn-Si alloy, revealed that it comprises eight elementary tetrahedra. The resulting elementary quaternary systems and their volumes are summarized in **Table 1.**

Table 1 List of tetrahedra of the Cr-Mn-Si-Fe metal system

№	Tetrahedron	Volume
1	Fe-Cr-Cr_3Si-Mn	0.160
2	Fe-Cr_3Si-Fe_2Si-Mn	0.159
3	Fe_2Si-Mn-Mn_5Si_3-Cr_3Si	0.150
4	Fe_2Si- Mn_5Si_3-MnSi-Cr_3Si	0.070
5	Fe_2Si-Cr_3Si-FeSi-MnSi	0.090
6	FeSi-Cr_3Si-Cr_5Si_3-MnSi	0.030
7	FeSi-Cr_5Si_3-$CrSi_2$-MnSi	0.130
8	FeSi-$CrSi_2$-Si-MnSi	0.210
Total		1.000

l phase composition diagrams obtained can be processed analytically without visualizing the system, yielding equations for exploring its physicochemical properties [21, 22]. There is a straightforward and manually calculable method for deriving transformation equations that express any secondary system through the primary components of the base system [21-25]. The criterion for locating a given composition of melts within one of the quasi-systems is the positive values of the n-th number of secondary components, determined by the polytope and calculated using Hize's equation.

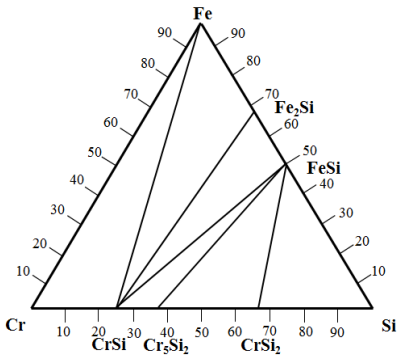

Fig. 1 Phase diagrams of the Fe-Cr-Si system

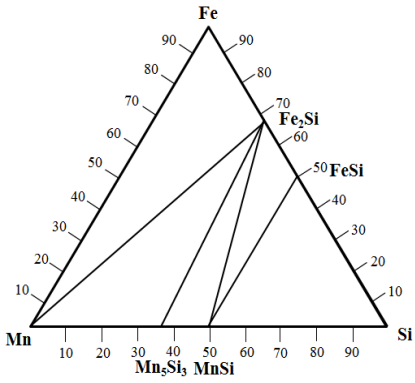

Fig. 2 Phase diagrams of the Fe-Mn-Si system

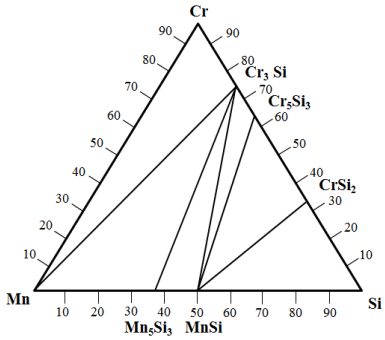

Fig. 3 Phase diagrams of the Cr-Mn-Si system

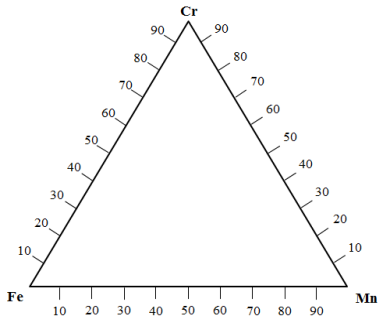

Fig. 4 Phase diagrams of the Cr-Mn-Fe system

THERMODYNAMIC MODELING RESULTS

Based on the aforementioned methods, coefficients were derived and calculated for each secondary component from the 8 quasi-systems of the base tetrahedron, presented in **Table 2**. **Fig. 5** depicts the resulting phase diagram of the four-component Cr-Mn-Si-Fe system, graphically represented as a tetrahedron. **Fig. 6** illustrates the tetrahedron modelling the composition of the smelting products.

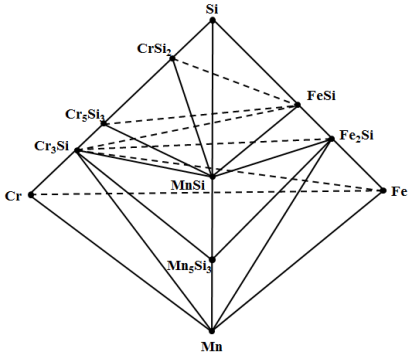

Fig. 5 Tetrahedration of the Cr-Mn-Si-Fe metal system

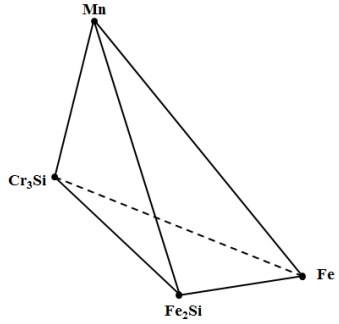

Fig. 6 Tetrahedron modelling the composition of melting products

It has been determined that the composition of the complex ferroalloy Fe-Cr-Mn-Si, derived from a mixture of chromium and manganese ores, is modelled by tetrahedron №2 (**Fig. 6**). This tetrahedron ranks second in relative volume among the eight identified tetrahedra. Consequently, the substantial volume of this tetrahedron provides the most favorable conditions for the smelting process, that is, the flexible regulation of the charge composition.

Table 2 List of elementary tetrahedra, their volumes, and coefficients for equations to calculate equilibrium relations of secondary components in the Cr-Mn-Si-Fe system

Initial components	Coefficients	Tetrahedra, their volumes and coefficients of transformation							
		1	2	3	4	5	6	7	8
		Fe-Cr-Cr_3Si-Mn	Fe-Fe_2Si-Cr_3Si-Mn	Mn_5Si_3-Fe_2Si-Cr_3Si-Mn	Mn_5Si_3-Fe_2Si-Cr_3Si-MnSi	FeSi-Fe_2Si-Cr_3Si-MnSi	FeSi-Cr_5Si_3-Cr_3Si-MnSi	FeSi-Cr_5Si_3-$CrSi_2$-MnSi	FeSi-Si-$CrSi_2$-MnSi
Volumes		0.160	0.159	0.150	0.070	0.090	0.030	0.130	0.210
Fe	a1	1.000	1.000	-1.070	1.610	-1.600	1.500	1.500	1.500
	a2	0	0	1.300	1.280	2.500	-4.600	0.800	-0.500
	a3	0	0	0	0	0	4.100	-1.400	0
	a4	0	0	0.820	-1.860	0	0	0	0
Cr	b1	0	0.720	-0.770	1.200	-1.100	0	0	0
	b2	1.000	-0.900	0	0	0.900	-1.700	1.900	-1.100
	b3	0	1.200	1.200	1.200	1.200	2.700	-0.880	2.100
	b4	0	0	0.590	-1,300	0	0	0	0
Mn	c1	0	0	0	3.300	-3.030	0	0	0
	c2	0	0	0	0	2.550	-4.690	0.890	-0.510
	c3	0	0	0	0	0	4.200	-1.400	0
	c4	1.000	1.000	1.000	-2.280	1.510	1.510	1.510	1.510
Si	d1	0	-4.000	4.280	-6.440	6.020	0	0	0
	d2	-5.580	5.000	0	0	-5.020	9.220	-1.750	1.000
	d3	6.580	0	0	0	0	-8.22	2.750	0
	d4	0	0	-3.280	7.440	0	0	0	0

The chronology of the movement of the relative compositions of the Fe-Cr-Mn-Si ferroalloy, with respect to their Cr and Mn content, occurs within the tetrahedron listed in **Table 3**.

Table 3 Calculated chemical composition of the Fe-Cr-Mn-Si ferroalloy obtained from a mixture of chromium and manganese ores and the list of tetrahedra in which they are located

Ferroalloy grade	Cr	Fe	Mn	Si	Tetrahedron	Volume
ΣCr+Mn=55%	27.25	30.16	27.35	9.8	Fe-Cr_3Si-Fe_2Si-Mn	0.17

Materials and methods of Fe-Cr-Mn-Si smelting

Laboratory smelting of the Fe-Cr-Mn-Si alloy was conducted using Kazakhstani chromium and low-grade manganese ores with coke as a reductant. The smelting processes were done in a high-temperature Tamman electric furnace with graphite heaters. The Tamman resistance furnace is a research installation designed to achieve high temperatures up to 2000 °C and simulates metallurgical processes. This high-temperature unit is equipped with a carbon-tube workspace and a heater operated by a power transformer. Temperature control in the furnace is smoothly managed using a thyristor voltage regulator connected to the primary winding of the power transformer, allowing for generating several thousand amps of current at low voltage on the output busbars (ranging from 0.5 to 15 V). The mixture of charge materials was placed in a graphite crucible with a diameter of 35 mm and a height of 110 mm. The heating rate was maintained at 15°C/min.

The charge materials were proportioned as follows: chromium ore – 41%, manganese ore – 41%, coke – 18%. This charge composition was selected to achieve a ferroalloy composition calculated based on thermodynamic modelling (**Table 3**) within tetrahedron No. 2 (**Fig. 6**).

Their chemical and technical compositions are detailed in **Table 4**.

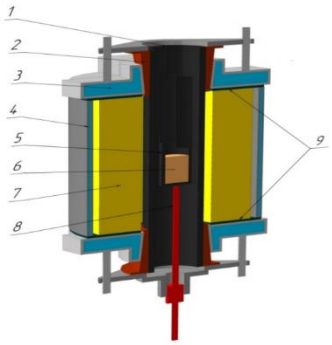

1 - graphite carbon tube; 2 – copper ring; 3,4 – lid and body with water cooling; 5 - crucible; 6 - charge under investigation; 7 – protective casing; 8 - thermocouple; 9 - insulating material.

Fig. 7 Tamman laboratory furnace (cutout view)

Table 4 The chemical and technical compositions of the charge materials

Material	Compound, %						
	$C_{тв}$	A^c	W^p	V^{daf}	SiO_2	Al_2O_3	MgO
Coke	84.39	13.79	0.28	1.84	—	—	—
Material	Compound, %						
	Cr_2O_3	Mn_{gen}	Fe_{gen}	CaO	SiO_2	Al_2O_3	MgO
Chrome ore	45.09	—	16.22	1.3	6.44	8.99	12.92
Manganese ore	—	17.88	5.16	0.98	41.3	5.92	2.25

The charge materials were fractionated to a particle size of less than 5 mm. The melting commenced within the temperature range of 1500-1600 °C, and the heat was raised to a temperature of 1700 °C, which was maintained for 40 minutes.

SMELTING RESULTS

Upon cooling, the metal and slag were easily separated from each other (**Fig. 8**). The chemical composition of the obtained metal and slag is presented in **Tables 5 and 6**, respectively.

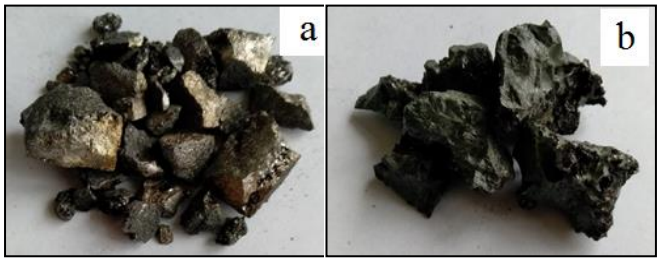

Fig. 8 – Appearance of the metal and slag obtained in the Tamman furnace: a – metal; b – slag

Table 5 – Chemical composition of the metal, %

Metal	Component, %					
	Cr	Fe	Mn	Si	C	S
	44.07	13.97	12.48	9.48	4.45	0.009

Table 6 – Chemical composition of slag, %

Slag	Component, %						
	Cr_2O_3	Al_2O_3	SiO_2	CaO	MgO	FeO	Mn_{gen}
	8.49	11.99	20.85	13.10	0.25	2.28	19.48

The metal fragments exhibited a characteristic metallic luster. The slag, upon cooling, was stone-like and solid.

Consequently, the laboratory crucible smelting results collectively suggest the feasibility of obtaining the complex Fe-Cr-Mn-Si alloy from a charge consisting of Kazakhstani chromium and low-grade manganese ores, using coke as the reductant. The extraction of components into the alloy was %: 42.5 Mn; 85.7 Cr; 20.8 Si; 23.8 Fe.

The laboratory crucible smelting results analysis indicated low Si and Mn extraction yields into the alloy – 20.8 and 42.5 %, respectively.

Thermodynamic modelling focuses on equilibrium states, but real-world systems often operate far from equilibrium. Some discrepancies between the composition of the obtained ferroalloy and the calculated composition can be explained by the fact that the smelting was conducted without a vacuum and inert gas supply. Consequently, the charge interacted with oxygen in the surrounding atmosphere during heating. Additionally, carbon was introduced as a fifth element in the charge.

Mn often has a high affinity for oxygen and can form stable oxides that are difficult to reduce. Si is known for forming strong bonds with oxygen, resulting in the formation of SiO_2, which is a refractory material with a high melting point. Cr typically has a lower affinity for oxygen than Mn, making its reduction easier and more complete. This is likely the reason for the high extraction rate of Cr. Therefore, the extraction rate of Si and Mn is typically lower than that of Cr. The formation of complex oxides containing Mn, Si and Fe may also contribute to a lower reduction rate.

It's important to note that the specific thermodynamic conditions within the Tamman furnace, such as temperature and atmosphere, play a crucial role in the reduction behavior of these elements. For example, high temperature enhances the reduction kinetics but also increases volatility of some elements, especially Mn and Si.

The kinetics of these processes can be significantly complex, as they involve solid-state reactions and gaseous diffusion. Low extraction is also attributed to the high volatilization of these elements into the gas phase due to the absence of a filtering layer of charge materials in ore thermal furnaces, where such alloys are more commonly performed [26, 27]. The presence of a significant amount of condensate in the furnace's graphite tube confirmed the substantial volatilization of the principal elements.

The obtained sample was microstructurally investigated using a scanning electron microscope (SEM), coupled with an analysis of its components by energy-dispersive spectroscopy (EDS). **Fig. 9** depicts microstructural images acquired using an SEM.

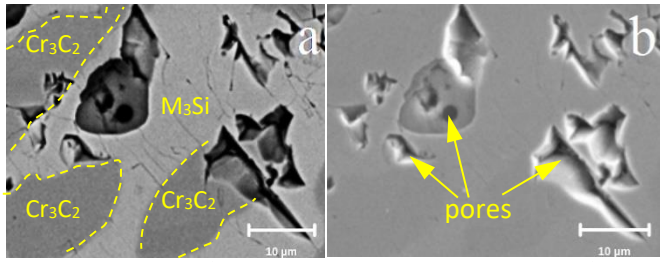

Fig. 9 – Microstructure of the obtained metal sample captured in the mode of detection: a – backscattered electrons; b – secondary electrons

The images provided allow for an analysis of the composition (the EDS results of the microstructure components are presented in **Table 7**) and topography of the microstructure. In the detection mode for backscattered electrons (**Fig. 9a**), the high atomic number elements are highlighted, showcasing the silicide matrix, indicated by the generalised formula M_3Si, where M refers to a combination of Cr, Fe, and Mn. The secondary electron mode (**Fig. 9b**) reveals the sample's topography, emphasising the material's physical texture and porosity characteristics.

Table 7 – EDS-analysis results (Figure 9a)

	Element, %				
Component	Fe	Cr	Mn	Si	C
M_3Si	31.74	48.91	10.99	8.35	-
Cr_3C_2	8.37	72.73	5.84	-	13.07

The microstructure demonstrates a dual-phase composition. The EDS analysis, summarized in **Table 7**, quantifies the elemental composition and corroborates the presence of a $(Cr, Fe, Mn)_3Si$ silicide phase alongside Cr_3C_2 carbide inclusions within the matrix. Porosity associated with gas release during the smelting process is also observed.

In the ferroalloy obtained, the silicide phase $(Cr, Fe, Mn)_3Si$ was observed, as predicted by thermodynamic modelling, which falls within the considered tetrahedron. Additionally, Cr_3C_2 formed, attributable to its high content in the ferroalloy composition and Cr high propensity for carbide formation.

The tendency of silicon to form silicides with other metals in a ferroalloy shows in the Mn > Fe > Cr sequence when considering the standard Gibbs free energy change involved in creating their respective silicides.

Cr and Fe tend to form carbides more than Mn, with Cr carbides being particularly stable. Si, while not a carbide former, affects the stability and formation of carbides in alloy systems due to its strong affinity for oxygen and its tendency to form silicides.

These characteristics elucidate the patterns of silicide and carbide formation in the microstructure.

CONCLUSION

The information and results of the calculations presented confirm the validity of the tetrahedron of the phase structure diagram for the Cr-Mn-Si-Fe metallic system. This will subsequently allow for determining the phase composition of metallic products during the smelting of various grades of the Fe-Cr-Mn-Si complex alloy.

1) Analytical equations were defined for each tetrahedron. With these equations, one can ascertain the positions of various metallic melt compositions in the factorial space of the overall system and calculate the standard phase composition of the melts under investigation.

2) Quasi-volumes in the Cr-Fe-Mn-Si system were identified, which alter the composition of metallic products when smelting different grades of Fe-Cr-Mn-Si. It was established that the composition of the complex Fe-Cr-Mn-Si alloy obtained from a mixture of chromium and low-grade manganese ores ($\sum$Cr+Mn=55%) is modelled by tetrahedron which provides the most favourable conditions for the smelting process.

3) An experimental smelting of Fe-Cr-Mn-Si was conducted in a high-temperature furnace, which yielded a sample with the following composition, %: 44.07 Cr, 13.97 Fe, 12.48 Mn, 9.48 Si, 4.45 C. The extraction of components from the raw materials was as follows, %: 42.5 Mn, 85.7 Cr, 20.8 Si, and 23.8 Fe. The microstructure comprises a complex silicide $(Cr, Fe, Mn)_3Si$ and Cr_3C_2 carbides.

Acknowledgement: This research is funded by the Science Committee of the Ministry of Education and Science of the Republic of Kazakhstan (Grant No. AP19676290).

REFERENCES

1. N. Sahu, A. Biswas, G. U. Kapure, N. S. Randhawa: Calphad, 66, 2019, 101637. https://doi.org/10.1016/j.calphad.2019.101637.
2. B. Abolpour, R. Shamsoddini: Progress in Reaction Kinetics and Mechanism, 45, 2020. https://doi.org/10.1177/1468678319891416.
3. V.I. Zhuchkov, O.V. Zayakin: KnE Materials Science, 5, 2019, 138–144. https://doi.org/10.18502/kms.v5i1.3961.
4. H. Cengizler, R.H. Eric: Silicon and Manganese Partition Between Slag and Metal Phases and Their Activities Pertinent to Ferromanganese and Silicomanganese Production. Proceedings of the *10th International Conference on Molten Slags, Fluxes and Salts*, Springer: Seattle, USA, 2016, pp. 1309-1317.
5. N. A. Andreev, V. I. Zhuchkov, O. V. Zayakin: Russian Metallurgy (Metally), 2013(6), 2013, 418–419. https://doi.org/10.1134/S0036029513060025.
6. O. Polyakov: Complex ferroalloys and other master alloys. In M. Gasik (Ed.), *Handbook of Ferroalloys*, Butterworth-Heinemann: Oxford, 2013, pp. 495–505. https://doi.org/10.1016/B978-0-08-097753-9.00020-4.
7. F. Rifat, et al.: Materials Letters, 116, 2014, 101–103. https://doi.org/10.1016/j.matlet.2013.10.105.
8 B. Smitirupa, et al.: Current Opinion in Green and Sustainable Chemistry, 26, 2020, 100377. https://doi.org/10.1016/j.cogsc.2020.100377.
9. M. Sommerfeld, B. Friedrich: Minerals, 11(11), 2021, 1286. https://doi.org/10.3390/min11111286
10. N.B. Duong, Q. Vu, T. Vu, C. Doan, H. Tran: Acta Metallurgica Slovaca, 27(3), 2021, 109–113. https://doi.org/10.36547/ams.27.3.948.
11. A. Glotka, S. Byelikov, O. Lysytsya: Acta Metallurgica Slovaca, 30(1), 2024, 15–18. https://doi.org/10.36547/ams.30.1.1991.
12. G.G. Mikhailov, L.A. Makrovets: Russian Metallurgy (Metally), 2023, 2023, 1159–1164. https://doi.org/10.1134/S0036029523080153.
13. H. Zhou, et al.: Calphad, 52, 2016, 110–119. https://doi.org/10.1016/j.calphad.2015.12.005.
14. Z.-K. Liu: Acta Materialia, 200, 2020, 745–792. https://doi.org/10.1016/j.actamat.2020.08.008.
15. A. Berche, J.-C. Tédenac, P. Jund: Calphad, 55, 2016, 181–188. https://doi.org/10.1016/j.calphad.2016.09.002.
16. J. Miettinen, S. Koskenniska, V.V. Visuri: Metallurgical and Materials Transactions B, 51, 2020, 2946–2962. https://doi.org/10.1007/s11663-020-01973-y
17. J. Aurélie, E. Povoden-Karadeniz: Calphad, 71, 2020, 101998. https://doi.org/10.1016/j.calphad.2020.101998.
18. J. Tranquillo: Thermodynamics of Complex Systems. *In An Introduction to Complex Systems*, Springer: Cham, 2019, 85-113. https://doi.org/10.1007/978-3-030-02589-2_7.
19. S.O. Baisanov, N.Z. Nurgali, M.S. Almagambetov: Industry of Kazakhstan, (4), 2008, 75–77.
20. A. Kh. Nurumgaliev, E. E. Kiekbaeva: Proceedings of the University of Karaganda, 11, 2008, 20–23.
21. B.K. Kasenov, M.K. Aldabergenov, A.S. Pashinkin, Sh.B. Kasenova, E.T. Balakeeva, S.M. Adekenov: *Methods of applied thermodynamics in chemistry and metallurgy*. Elasir: Karaganda, 2008.
22. Ye.Zh. Shabanov: *Development of technology for smelting aluminosilicon oxide from high-solid coals of the Karaganda basin and screenings of high-carbon ferrous oxide*. Doctoral dissertation, Karaganda Technical University, 2016. https://www.kstu.kz/o-zashhite-doktorskoj-dissertatsii-shabanova-erbola-zha-syly-ly/
23. Ye.N. Makhambetov: *Development of technology for smelting complex calcium-containing ferroalloys from waste metallurgical slags and high-ash coals*. Doctoral dissertation, Karaganda Technical University, 2021. https://www.kstu.kz/260370/

24. E.K. Mukhambetgaliev, V.E. Roshchin, S.O. Baisanov: Izvestiya: Ferrous Metallurgy, 61(7), 2018, 564–571 (in Russian). https://doi.org/10.17073/0368-0797-2018-7-564-571.
25. A.A. Akberdin: KIMS, 3, 1995, 92–93.
26. V. Shevko, Y. Afimin, G. Karatayeva, A. Badikova, T. Ibrayev: Acta Metallurgica Slovaca, 27(1), 2021, 23–27. https://doi.org/10.36547/ams.27.1.745.
27. N. Vorobkalo, A. Baisanov, Y. Makhambetov, Y. Myn-zhasar, N. Nurgali: Heliyon, 9(8), 2023, e18989. https://doi.org/10.1016/j.heliyon.2023.e18989.